无 机 化 学 学 报

2018 年　　第 34 卷　　第 2 期

目　次

论　文

CHINESE JOURNAL OF INORGANIC CHEMISTRY

Vol.34 No.2 Feb. 2018

CONTENTS

Cover

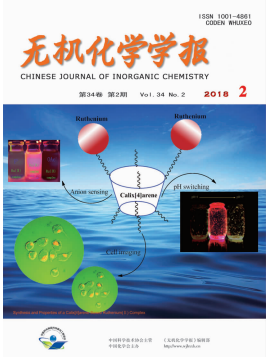

Articles

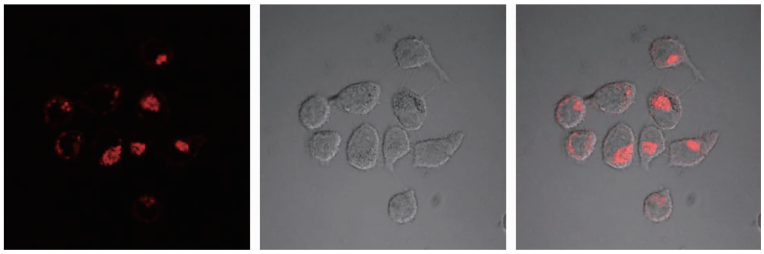

A new calix[4]arene-based ruthenium(Ⅱ) complex **1** was synthesized and characterized, which can acts as pH-induced "off-on-off" luminescence switches (I_{on} / I_{off}= 1.42 and 96.0), "turn off" emission sensor for F^- and OAc^-, and can rapidly penetrate through the HeLa cells membrane with low cytotoxicity at the imaging concentration.

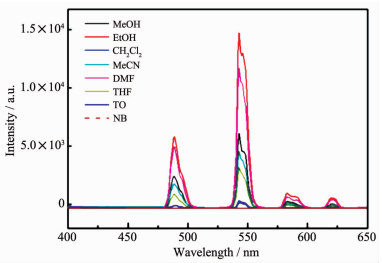

The luminescence intensity of Tb-MOF can be modulated by organic small molecule solvents, and Tb-MOF exhibited the significant quenching in nitrobenzene.

Four Cadmium-Organic Coordination Polymers: Influence of Secondary Ligands to Crystal Structure and Luminescent Properties

ZHANG Shu-Quan, ZHANG Jian-Han, GU Jia-Fang

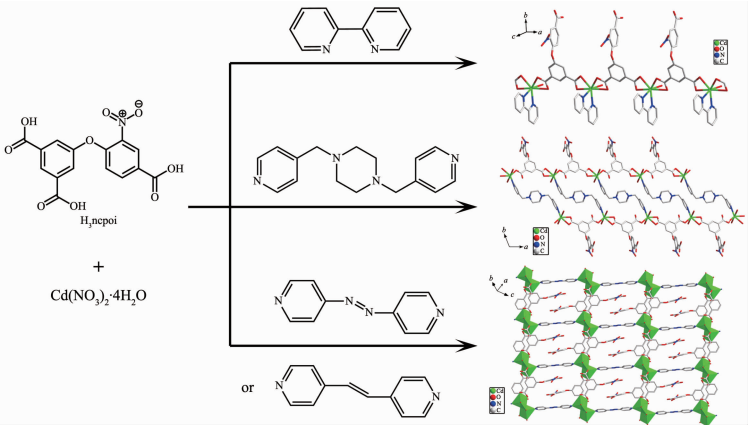

DOI:10.11862/CJIC.2018.039
Chinese J. Inorg. Chem., **2018**,**34**(2):237-246

Preparation and Electrochemical Properties of $(Pr_{0.9}La_{0.1})_2(Ni_{0.74}Cu_{0.21}Ga_{0.05})O_{4+\delta}$ Nanofiber Cathode

SHENG Shuang, ZHAO Jia-Qi, SUN Li-Ping, HUO Li-Hua, ZHAO Hui

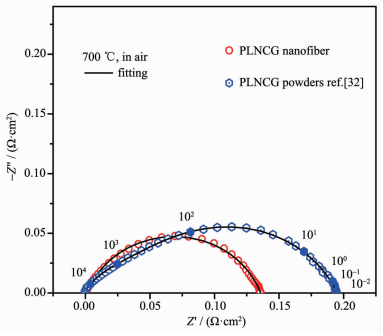

The ORR of $(Pr_{0.9}La_{0.1})_2(Ni_{0.74}Cu_{0.21}Ga_{0.05})O_{4+\delta}$ nanofiber cathode has been greatly improved. The polarization resistance (R_p) of the nanofiber cathode is 0.134 Ω·cm² at 700 ℃ in air, which is 32% less than the PLNCG powder cathode (R_P=0.197 Ω·cm²).

DOI:10.11862/CJIC.2018.043
Chinese J. Inorg. Chem., **2018**,**34**(2):247-254

Preparation and Photoelectric Performance of CdTe/CdS Co-sensitized TiO_2 Electrode Materials

WANG Jie, JI Ya-Jun, DENG Ya-Lei, ZHOU Lu-Wei

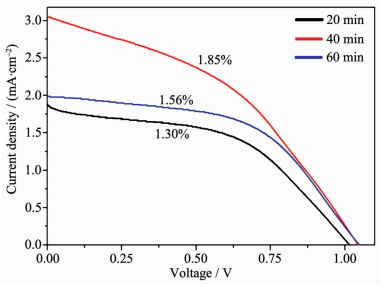

Under optimal condition, the short circuit photocurrent density and photoelectric conversion efficiency of CdS/CdTe/TiO_2 could reach up to 3.1 mA·cm^{-2} and 1.85%, respectively.

DOI:10.11862/CJIC.2018.051
Chinese J. Inorg. Chem., **2018**,**34**(2):255-262

Synthesis of $LiFePO_4$/C Composites Using $Fe_2P_2O_7$ as Precursor by a Two-Setp Solid-State Method (English)

WANG Yao, LI Yan-Cheng, FENG Li-Yuan, ZHAO Qiang, WANG Gui-Xin, LUO Chun-Hui, YAN Kang-Ping

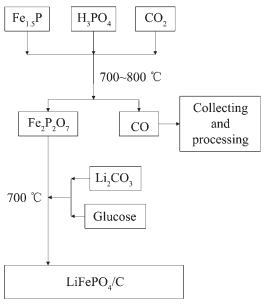

$Fe_2P_2O_7$ was prepared by a solid-state method from $Fe_{1.5}P$ slag, CO_2 and H_3PO_4, and it′s furtherly used as precursor of $LiFePO_4$/C composites. This work puts forward a novel low-cost, environmentally friendly (CO_2 consuming) and simplified method for synthesis $Fe_2P_2O_7$ precursor for $LiFePO_4$.

DOI:10.11862/CJIC.2018.044
Chinese J. Inorg. Chem., **2018**,**34**(2):263-269

Alkoxy Phenanthrolines: Design and Synthesis and Heteroleptic Copper Complexes as Photosensitizers in Water Reduction for Hydrogen Production

WU Qing-An, CHEN Hao, HUANG Dao-Chen, XIA Liang-Min, WANG Xiao-Jing, LOU Wen-Ya, WU Xiao-Feng, LUO Shu-Ping

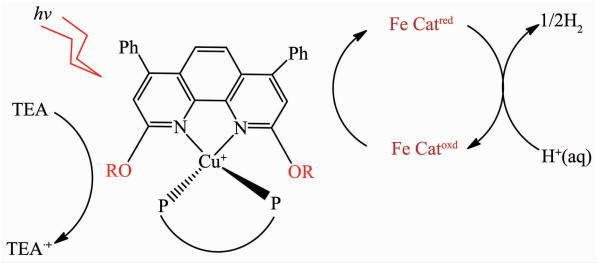

Novel alkoxy phenanthrolines photosensitizers

DOI:10.11862/CJIC.2018.057
Chinese J. Inorg. Chem., **2018**,**34**(2):270-276

Synthesis, Structure, and Properties of Zintl Phase Compound α-$BaZn_2P_2$ (English)

BAI Ming-Cheng, PAN Ming-Yan, WANG Lin, QI Hong-Ji, WANG Hu

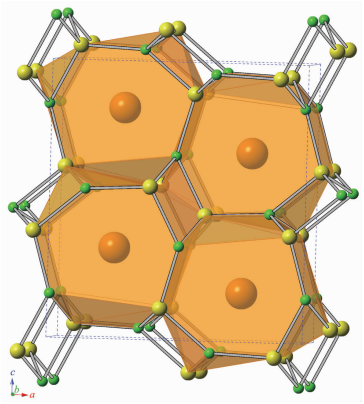

The α-$BaZn_2P_2$ (*Pnma*) has a three-dimensional network structure where ZnP_4 tetrahedra form an anion frame by sharing sides or vertices and it owns the energy gap of 0.4 eV.

DOI:10.11862/CJIC.2018.056
Chinese J. Inorg. Chem., **2018**,**34**(2):277-282

Lead/Rare Earth-Free Green-Light-Emitting Crystal of Molecular-Based Hybrid Compound: $(C_5H_{13}ClN)_2[MnCl_4]$ with Large Crystal Size (English)

CAI Xing-Wei, QIANG Wei, ZHAO Yu-Yuan, LI Hong, HUANG Cui-Ping, GUO Yong-Chun

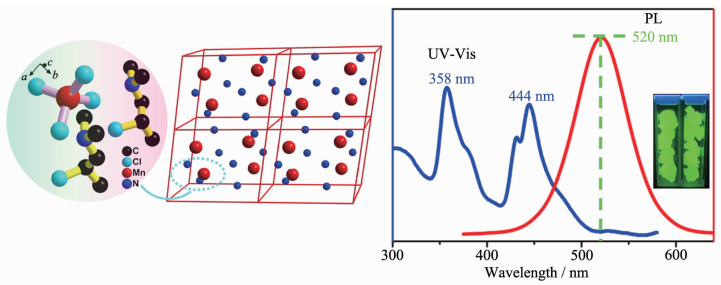

The novel molecular compound $(C_5H_{13}ClN)_2[MnCl_4]$, which possesses intense greenish fluorescent emission (520 nm) and high thermal stability, would pave a way to fabricate high-performance emitting devices.

DOI:10.11862/CJIC.2018.068
Chinese J. Inorg. Chem., **2018**,**34**(2):283-288

Effect of Ag-Doping on the Structural and Photoluminescence Properties of n-ZnO Nanorods/p-GaN Heterojunction

YU Chun-Yan, HU Fang, MEI Fu-Hong, LI Rui, JIA Wei, LI Tian-Bao

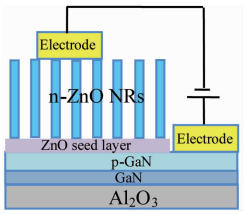

With increasing Ag doping, the near band edge emission peak of Ag-doped ZnO nanorods shows a redshift, its intensity weakened gradually, and n-ZnO nanorods/p-GaN heterojunction will have better conductivity.

DOI:10.11862/CJIC.2018.033
Chinese J. Inorg. Chem., **2018**,**34**(2):289-294

High-Yield Synthesis and Isomeric Ratio Control of La Endohedral Metallofullerenes

SUN Chang, ZHAO Sha-Sha, CHEN Ying, CHEN Mu-Qing, XIE Yun-Peng, LU Xing

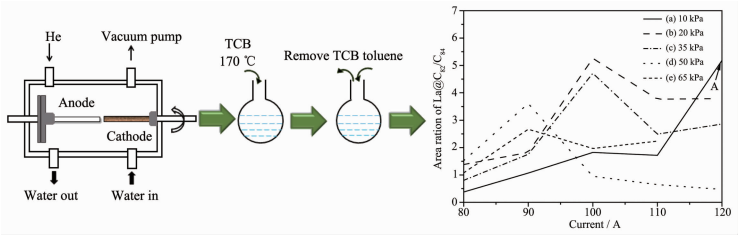

DOI:10.11862/CJIC.2018.031
Chinese J. Inorg. Chem., **2018**,**34**(2):295-299

The production yield of $La@C_{82}$ and $La_2@C_{80}$ was investigated in detail by considering the synergistic effect of He pressure and current density in the arc-discharge process. The results showed the yield of $La@C_{82}$ and $La_2@C_{80}$ can be significantly increased, and the relative abundance of $La@C_{82}$ isomers can also be adjusted.

Hierarchical SAPO-34: Synthesis and Catalytic Performances in Methanol to Olefins

CUI Xing-Yu, WANG Jing-Jing, PAN Meng, NING Wei-Wei, YAN Lin-Lin, ZHENG Jia-Jun, LI Rui-Feng

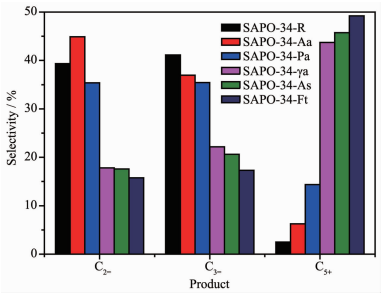

DOI:10.11862/CJIC.2018.046
Chinese J. Inorg. Chem., **2018**,**34**(2):300-308

Nanocrystals or the created hierarchical pore system in SAPO-34 resulted in shortened microporous channels, which not only gave a prolonged catalytic life, but also conttributed to enhancing the selectivitity for the oil by alleviating the formation of olefin in the products during methanol to olefins process.

Binuclear Cobalt(Ⅱ) and Nickel(Ⅱ) Complexes with *o*-Aminophenol Schiff Base: Syntheses, Structures, Antitumor Activity and Quantum Chemistry Calculation

XIE Qing-Fan, GUO Miao-Li, CHEN Yan-Min

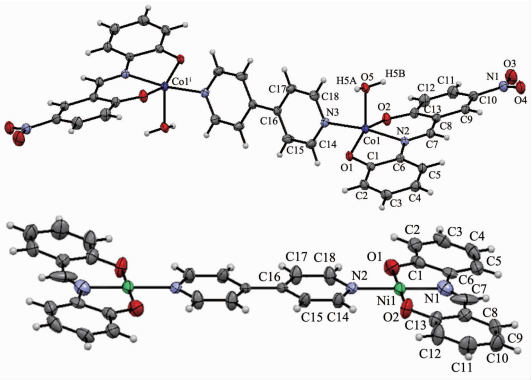

DOI:10.11862/CJIC.2018.028
Chinese J. Inorg. Chem., **2018**,**34**(2):309-316

Mn^{4+} Doped Co_3O_4 Nanofibers: Preparation by Electro-Spinning and Electrochemical Performance

ZHU Ya-Bo, TANG Xiao-Tong, DUAN Lian-Wei, LIU Wan-Ying, CAO Xing-Xing, FENG Pei-Zhong

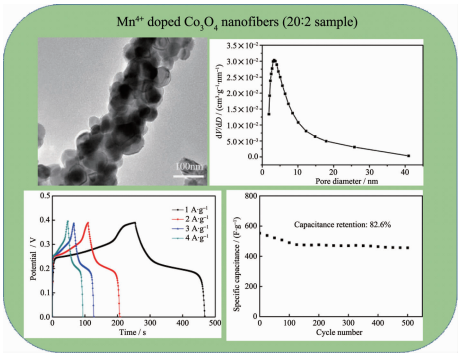

DOI:10.11862/CJIC.2018.030
Chinese J. Inorg. Chem., **2018**,**34**(2):317-324

Preparation and Luminescent Properties of Eu^{3+} Doped B_2O_3-CaO Luminescent Materials

CAO Jiao-Lan, WANG Xi-Gui

DOI:10.11862/CJIC.2018.066
Chinese J. Inorg. Chem., **2018**,**34**(2):325-330

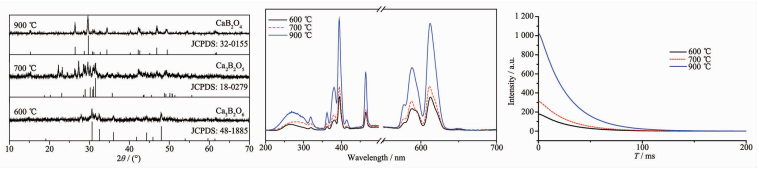

The high pure CaB_2O_4:Eu^{3+} phosphor obtained by annealing at 900 ℃ has the best luminescence performance and the longest fluorescence decay time, which is attributed to the fact that Eu^{3+} in the matrix is more likely to replace Ca^{2+} to form relatively large numbers of p-n junctions and traps.

Fabrication and Characteristics of Thermoelectric Microgenerators Based on Single Sb Doped ZnO Microwire

FENG Qiu-Ju, SHI Xiao-Chi, XING Yan, LI Fang, LI Tong-Tong, PAN De-Zhu, LIANG Hong-Wei

DOI:10.11862/CJIC.2018.042
Chinese J. Inorg. Chem., **2018**,**34**(2):331-336

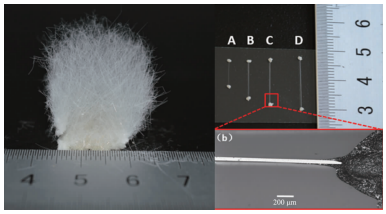

Large-scale Sb doped ZnO microwire arrays were grown by chemical vapor deposition method without using metal catalyst. The devices can produce a maximum output voltage of about 36 mV, a maximum output power of about 10.8 nW. The single Sb-doped ZnO microwires show a Seebeck coefficient of about −1.80 $mV \cdot K^{-1}$.

Core-Spacer-Shell Structured Fe_3O_4@MoO_3@$mSiO_2$ Nanocarrier: Preparation and Controlled Release Drug

TANG Guan-Xin, PENG Hong-Xia, HU Chuan-Yue, PENG Yang-Xi

DOI:10.11862/CJIC.2018.041
Chinese J. Inorg. Chem., **2018**,**34**(2):337-345

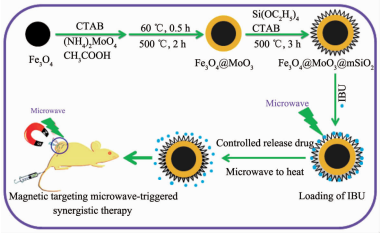

Schematic illustration of creating Fe_3O_4@MoO_3@$mSiO_2$ nanoparticles and microwave-triggered release drug

The dissertation constructed a novel MoO_3 interlayered Fe_3O_4@MoO_3@$mSiO_2$ core-spacer-shell structured nanoparticles to investigate loading and controllable release properties of ibuprofen (IBU). It has high surface area, large accessible pore volume, strong magnetic and unique microwave heating conversion behavior. The nanoparticles are feasibly applicable to simultaneous target drug delivery and microwave-triggered synergistic cancer therapy.

Syntheses, Crystal Structures and Photophysical Properties of Ionic Iridium(Ⅲ) Pyrimidine Complexes

WANG Ying, WEI Chuan-Dong, GE Guo-Ping, WANG Sui, LIANG Yun-Xiao

DOI:10.11862/CJIC.2018.048
Chinese J. Inorg. Chem., **2018**,**34**(2):346-352

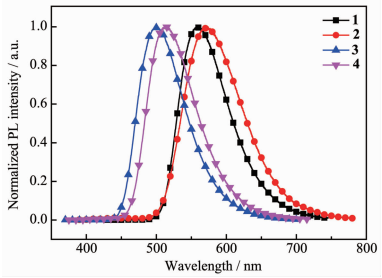

Four ionic iridium(Ⅲ) pyrimidine complexes exhibits yellow-green or green phosphorescent emission in CH_2Cl_2 with quantum efficiencies between 6.7% and 64.0%.

Chiral Supramolecular Liquid Crystal Based on Polyoxometalate

LI Zhi-Jun, ZHANG Jing, WEI Xue-Hong,
CAI Jin, WU Li-Xin

DOI:10.11862/CJIC.2018.050
Chinese J. Inorg. Chem., **2018**,**34**(2):353-358

Chiral nano-hybrid liquid crystal was achieved by the encapsulation of polyoxometalate with chiral mesomorphic promoters via electrostatic interactions.

Visible-Light Catalytic Performance of Rare Earth Ions Tm^{3+} Doped Bi_2WO_6

ZHAO Wei-Di, HE Jin-Yun, WANG Yan-Wu,
LONG Fei, PENG Dai-Jiang, ZOU Zheng-Guang

DOI:10.11862/CJIC.2018.062
Chinese J. Inorg. Chem., **2018**,**34**(2):359-366

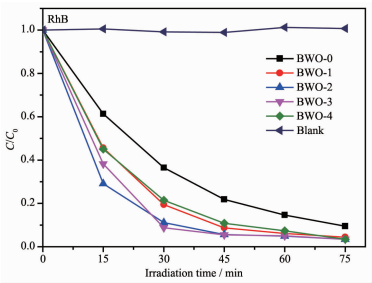

The rare earth Tm^{3+} doped Bi_2WO_6 photocatalysts were obtained by hydrothermal method. The main properties of the samples were investigated by PL. As a result, the sample had excellent degradation properties for rhodamine B and caramel.

Hydrothermal Synthesis of Mn(Ⅱ) Complex Based on Imidazole Ligand: Structure, Theoretical Calculation and Third-Order Nonlinear Optical Properties (English)

ZHANG Zai-Chao, TANG Guo-Dong,
TANG Ting-Ting, Lance F. Culnane, ZHANG Yu,
SONG Ying-Lin, LI Rong-Qing, XIA Min

DOI:10.11862/CJIC.2018.054
Chinese J. Inorg. Chem., **2018**,**34**(2):367-374

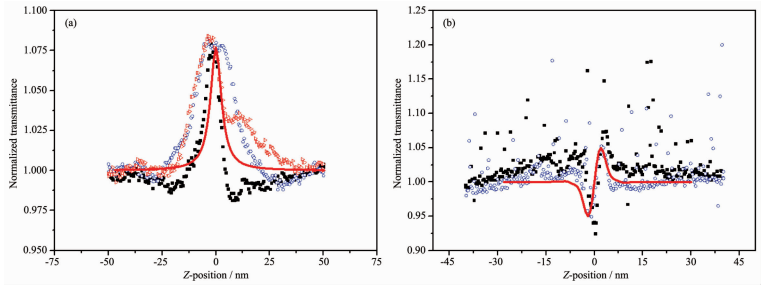

The complex exhibiting reverse saturable absorption has self-focusing property and strong excited-state absorption.

Crystal Structures and Fluorescence Property of Zn(Ⅱ)/Cd(Ⅱ) Complexes Based on *N*-((quinolin-8-yl)methylene) acetohydrazide (English)

XU Zhi-Hong, WU Wei-Na, LIU Shu-Yang, KOU Kai, WANG Yuan

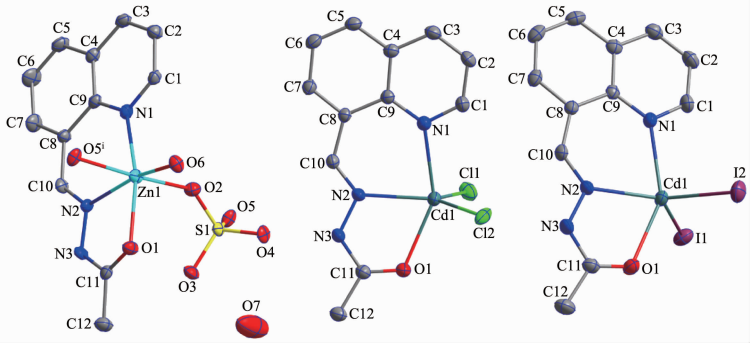

Three complexes $\{[Zn(HL)(H_2O)(SO_4)]\cdot H_2O\}_n$ (**1**), $[Cd(HL)Cl_2]$ (**2**) and $[Cd(HL)I_2]$ (**3**) with *N*-((quinolin-8-yl)methylene)acetohydrazide have been synthesized and characterized. The complexes **1** and **2** exhibit strong fluorescence emission probably due to a CHEF effect, while **3** is non-emissive because of the heavy atom effect of the coordinated iodide anions.

DOI:10.11862/CJIC.2018.032
Chinese J. Inorg. Chem., **2018**,**34**(2):375-380

Syntheses, Characterization and Luminescent Properties of Silver(I) Complexes Based on Diphosphine Ligands (English)

WANG Yu, CUI Yang-Zhe, LIU Min, WANG Meng-Qin, GENG Wen-Xiao, LI Zhong-Feng, JIN Qiong-Hua

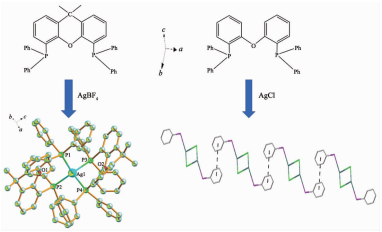

Complex **1** is a mononuclear complex, which was generated by the reaction of $AgBF_4$ and XANTphos with dmp (neocuproine). While, in complex **2**, taking the effect of $\pi\cdots\pi$ weak interactions into consideration, adjacent molecules are connected to form a 1D infinite chain.

DOI:10.11862/CJIC.2018.034
Chinese J. Inorg. Chem., **2018**,**34**(2):381-386

Mononuclear Assemblies with Metal-Metal Interaction: Syntheses and Catalytical Performance in Suzuki-Coupling Reaction (English)

HU Zhi-Yong, DENG Wei, LU Hong-Lin, HUANG Hai-Ping, YU Shu-Yan

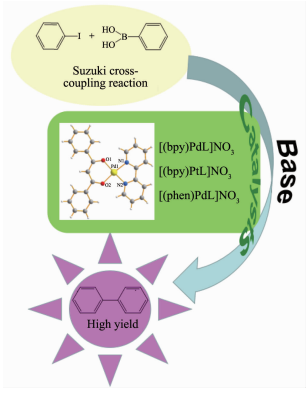

DOI:10.11862/CJIC.2018.036
Chinese J. Inorg. Chem., **2018**,**34**(2):387-396

Ag-$NaTaO_3$-RGO Composite: Synthesis and Improved Photocatalytic Hydrogen Production Property (English)

HE Hui-Juan, ZHANG Bin, ZHONG Zi-Jun, TAN Shao-Zao, HUANG Lang-Huan

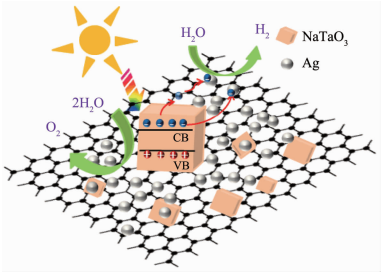

We have designed a new type of ternary photocatalyst with $NaTaO_3$, RGO and Ag. This Ag-$NaTaO_3$-RGO photocatalyst exhibits improved photocatalytic hydrogen production property. Among all the Ag-$NaTaO_3$-RGO samples, the 0.2Ag-$NaTaO_3$-RGO exhibits the highest hydrogen production rate (395 μmol·h^{-1}).

DOI:10.11862/CJIC.2018.015
Chinese J. Inorg. Chem., **2018**,**34**(2):397-403

Syntheses and Crystal Structures of Two Homogeneous Organic-Inorganic Compounds Based on $PbBr_2$ (English)

YUAN Guo-Jun, LIU Guang-Xiang, LIU Shao-Xian, MA Yun

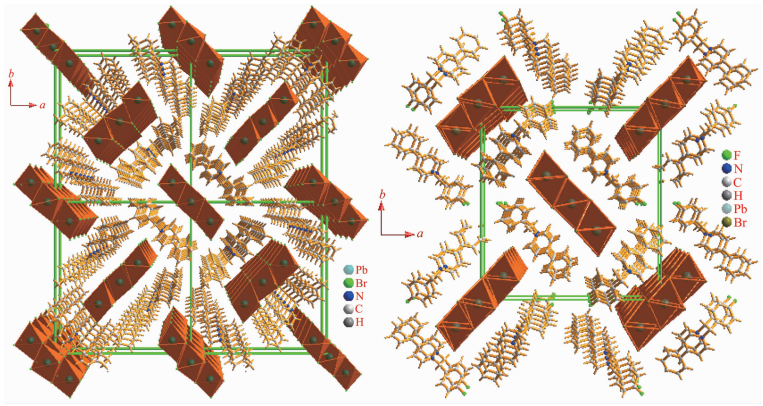

The results show that haloplumbate ion exhibits octahedron topology in compounds **1** and **2**, and all these octahedron topologies formed 1D $[Pb_3Br_9]_n$ polymeric chain through edge-sharing connecting modes.

DOI:10.11862/CJIC.2018.055
Chinese J. Inorg. Chem., **2018**,**34**(2):404-408

Preparation of Platinum Nanoparticles via Electrochemical Method in *N*,*N*-diethyl-*N*-methyl-*N*-(2-methoxyethyl)ammonium tetrafluoroborate Ionic Liquid (English)

WANG Dan, LIU Li-Lai, LI Ming-Xian, PAN Xiao-Na, ZHAO Yan-Hong, ZHANG Jin-Qiu, AN Mao-Zhong, YANG Pei-Xia

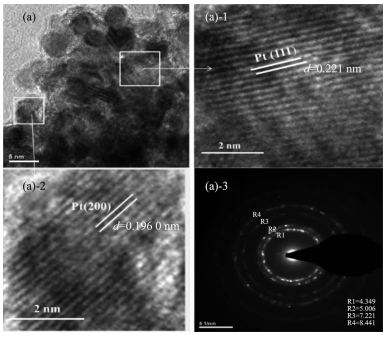

The HRTEM image of Pt nanoparticles demonstrates clear lattice fringes with an inter fringe distance of 0.221 and 0.196 nm corresponding to the lattice spacing of Pt(111), (200) planes, respectively. Its SAED pattern also reveals the face-centered cubic (fcc) Pt crystal structure.

DOI:10.11862/CJIC.2018.045
Chinese J. Inorg. Chem., **2018**,**34**(2):409-414